Revista Mexicana de Astronomía y Astrofísica, **50**, 255–270 (2014)

A MID INFRARED STUDY OF LOW-LUMINOSITY AGNS WITH WISE

R. Coziol,[1] J. P. Torres-Papaqui,[1] I. Plauchu-Frayn,[2] H. Andernach,[1] D. M. Neri-Larios,[3]
R. A. Ortega-Minakata,[1] and J. M. Islas-Islas[1]

Received 2014 January 26; accepted 2014 May 16

RESUMEN

Utilizando datos en el infrarrojo medio (MIR) del Wide-field Infrared Survey Explorer (WISE), mostramos que las galaxias AGNs de baja luminosidad (LLAGNs) presentan colores en el infrarrojo medio (MIR) significamente diferentes de los de las estrellas post-rama asintótica gigante (PAGBs). Esto se debe a una diferencia en la distribución de energía espectral (SED), pues los LLAGNs muestran una componente plana debida a un AGN. Congruentemente con esta interpretación, mostramos que en un diagrama color-color los LINERs y las Seyfert 2s siguen una ley de potencia con colores específicos que permiten distinguir unas de las otras, y de las galaxias con formación estelar, en base a sus diferentes niveles de formación reciente de estrellas. Basado en estos resultados, presentamos un nuevo diagrama de diagnóstico en el MIR que confirma la clasificación obtenida en el óptico a partir de diagramas de diagnóstico estándar, e identifican claramente los LINERs y LLAGNs como verdareros AGNs.

ABSTRACT

Using data from the Wide-field Infrared Survey Explorer (WISE) we show that the mid infrared (MIR) colors of low-luminosity AGNs (LLAGNs) are significanlty different from those of post-asymptotic giant branch stars (PAGBs). This is due to a difference in the spectral energy distribution (SEDs), the LLAGNs showing a flat component due to an AGN. Consistent with this interpretation we show that in a MIR color-color diagram the LINERs and the Seyfert 2s follow a power law with specific colors that allow to distinguish them from each other, and from star forming galaxies, according to their present level of star formation. Based on this result we present a new diagnostic diagram in the MIR that confirms the classification obtained in the optical using standard diagnostic diagrams, clearly identifying LINERs and LLAGNs as genuine AGNs.

Key Words: galaxies: active — infrared: galaxies

1. INTRODUCTION

Studies of clusters and compact groups (Phillips et al. 1986; Coziol et al. 1998; Miller et al. 2003; Martínez et al. 2008, 2010) have revealed that many narrow emission-line galaxies (NELGs) cannot be classified using standard diagnostic diagrams (Baldwin, Phillips, & Terlevich 1981; Veilleux & Osterbrock 1987), because the most important emission lines, Hβ and [OIII]λ5007, are either too weak or not observed. This is rather common, affecting about 20% of the early-type galaxies in compact groups, but reaching 60% in clusters (Phillips et al. 1986; Coziol et al. 1998; Miller et al. 2003; Martínez et al. 2008).

After subtracting a stellar population template from their spectra, Coziol et al. (1998) have demonstrated that these unclassified NELGs have spectral characteristics typical of low luminosity AGNs: the emission lines have small equivalent widths (EWs), consistent with low emission luminosities, and the ratios [NII]λ6584/Hα are high, which is a defining trait of AGNs (Baldwin, Phillips, & Terlevich 1981; Veilleux & Osterbrock 1987; Osterbrock 1989). Subsequently, Martínez et al. (2008) confirmed that even after correcting for dust extinction the median value of the Hα luminosity in these galaxies is only 7.1×10^{39} erg s^{-1}, which qualify them as low-luminosity AGNs (LLAGNs; Ho, Filippenko, & Sargent 1997; Zhang, Dultzin-Hacyan, & Wang 2007; Martínez et al. 2008, 2010).

The most straightforward interpretation for LLAGNs is that they are some sort of evolved AGNs or "dying quasars", where matter at the center of the galaxies is falling on the exhausted accretion disk of a super-massive black hole (BH), reviving its activity (Coziol et al. 1998; Richstone et al. 1998; Miller

[1]Departamento de Astronomía, Universidad de Guanajuato, Guanajuato, Mexico.
[2]Instituto de Astronomía, Universidad Nacional Autónoma de México, Ensenada, B.C., Mexico.
[3]School of Physics, The University of Melbourne, Australia.

et al. 2003; Gavignaud et al. 2008). However, an alternative interpretation, put forward by Stasińska et al. (2008) and Cid Fernandes et al. (2010, 2011), suggests these galaxies are "retired galaxies", falsely identified as AGNs, in which the gas is ionized by post-asymptotic giant branch stars (PAGBs; Binette et al. 1994, hereafter the PAGB hypothesis). During the last few years, the PAGB hypothesis has won in popularity and was even proposed (e.g. Eracleous, Hwang, & Flohic 2010; Singh et al. 2013) to explain the LINERs, the prototype LLAGN that forms about 30% of all the early-type spiral galaxies observed in the field (Heckman 1980; Kauffmann 2009).

However, the PAGB hypothesis is somewhat ambiguous. The whole evolution from the AGB to the white dwarf phase cannot last more than 10000 years (Volk & Kwok 1989). This is a transient phenomenon that does not fit well with the ubiquity of the LLAGNs. It is not clear either to what phase of the post AGB evolution the PAGB hypothesis is alluding. By definition, an AGB is a red giant star that does not produce ionizing photons. When this star collapses, transforming into a white dwarf, the central star, for a brief period, becomes extremely hot, its effective temperature reaching up to 10^5 K (McCook & Sion 1999; Eisenstein et al. 2006). Sometime during this transformation, the star emits ultraviolet photons that are responsible for ionizing the gas of the envelope recently ejected from the AGB. This phase corresponds to that of the planetary nebula (PN). After that, the effective surface temperature of the central star falls down rapidly to about 10^4 K, which is not hot enough to ionize the gas. The expanding gas cloud thus becomes invisible, ending the PN phase (Kwok 2000). The star is now a white dwarf.

Strictly speaking, therefore, a PAGB is a pre-planetary nebula (pre-PN, see definition in Davies et al. 2005, Suárez et al. 2006, Kitsikis 2007), which describes the stage when the temperature of the evolving AGB is still rising, and that lasts only a few thousand years (Volk & Kwok 1989). Sometime during this brief phase the UV photons from the hot white dwarf would be able to escape from the expanding gas and dust envelope of the AGB and ionize the interstellar gas over a kpc region. The exact mechanism by which this is possible remains, however, largely unexplained (Binette et al. 1994). In spite of this problem, Taniguchi et al. (2000) claimed that it is not the pre-PN stars that ionize the gas in a galaxy, but the central hot white dwarfs of the PNs themselves. However, this would imply that the gas nebulae are generally optically thin, which means that all the PNs are density-bound. This is an oversimplification of the PN theory (see the basic explanations in Osterbrock & Ferland 2006). Moreover, this complicates the PAGB hypothesis, because one needs then to establish what fraction of the ionizing photons are escaping the nebulae. Consequently, the fluxes of UV photons required to ionize the gas might not be sufficient to explain a typical LLAGN. This is unless we have a very high number of PNs at all times, which is highly improbable considering the short lifetime of this phenomenon.

Nevertheless Stasińska et al. (2008), have claimed that both PAGBs (it is not clear if the authors refer to pre-PNs, PNs or both) and white dwarfs are responsible for producing the photons that can ionize the gas in LLAGNs over kpc regions. The ad hoc addition of white dwarfs to the PAGB hypothesis is interesting. White dwarfs can be present in great numbers in very old galaxies, which is the case of most LLAGNs (Torres-Papaqui et al. 2013), and they can live for a very long time. However, strictly speaking, we would call this model the "hot white dwarfs hypothesis", because only white dwarfs with an effective temperatures above 18000 K can produce ionizing photons (Bianchi et al. 2011). Again, this restriction might significantly reduce the available flux of ionizing photons in a LLAGN, considering that the majority of white dwarfs are cold, having a surface temperature well below 18000 K (McCook & Sion 1999; Eisenstein et al. 2006; Bianchi et al. 2011).

Taking into account the three possible "post AGB" phases as described above, there is one clear and immediate consequence of the PAGB hypothesis, which is that one would need a very high number of "hot PAGBs" to ionize the amount of gas observed in a typical LLAGN. In Binette et al. (1994, see their Table 1), the 15 galaxies for which the PAGB hypothesis was proposed have a mean Hα luminosity of $10^{39.6}$ erg s^{-1} (converting their cosmology to the one we used). In Martínez et al. (2008) an average luminosity of $10^{39.8}$ erg s^{-1} is reported for the LLAGNs (about 100 galaxies) in compact groups. In comparison, the 43922 LLAGN candidates in our present sample have an Hα luminosity that varies between 10^{41} and 10^{39} erg s^{-1}. Adopting 10^{40} erg s^{-1} for the mean Hα luminosity and using the equation $Q_H \sim 7.3 \times 10^{11} L_\alpha$ photon s^{-1} for the relation between the flux of ionizing photons, Q_H, and the Hα luminosity, L_α (Pottasch 1965; Kennicutt et al. 1994; Madau et al. 1998), we deduce that a flux of $10^{51.9}$ photon s^{-1} is needed to explain the ionized gas in a typical LLAGN. In Figure 1 of Binette et al. (1994) the normalized flux of ionizing photons produced by the PAGBs after about 13 Gyrs is predicted to be 10^{41} photon s^{-1} $M_\odot^{-1}$, which gives a mass of stars equal to $10^{51.9}/10^{41} = 10^{10.9} M_\odot$. Since the central star of a PAGB is a hot white dwarf with a mass $\sim 1 M_\odot$, this implies that of the order 10^{11} hot PAGBs are needed to ionize the gas in a typical LLAGN. Note that one obtains exactly the same number of white dwarfs using the model of Stasińska et al. (2008). Therefore, between 10^{12} and 10^{10} hot white dwarfs would be re-

quired by the PAGB hypothesis to explain the ionized gas in the LLAGN candidates forming our sample.

The fact that we need such a high number of white dwarfs is easy to understand. According to Coziol, Barth & Demers (1995) the equivalent of 10^5 O and B stars would be needed to ionize the gas in an average LLAGN (note that the same number of O and B stars is predicted after 10^7 yrs by the model of Binette et al. 1994). Because the number of ionizing photons emitted by a star is directly proportional to its surface area, which for a typical white dwarf is only 10^{-6} times that of a normal O star, then of the order of $10^5/10^{-6} = 10^{11}$ white dwarfs are thus required.

Obviously, like the massive stars in the SFGs, such a high number of hot white dwarfs in the LLAGNs must leave their trace elsewhere than in the optical spectra. In particular, it should be possible to test directly the PAGB hypothesis for the LLAGNs in the mid infrared (MIR; e.g. Pastoriza et al. 2000). The MIR emission is due to dust, which in a galaxy is either heated by stars or an AGN (Wright et al. 2010; Jarrett et al. 2011; Mateos et al. 2013; Assef et al. 2013). Since these two sources have different spectral energy distributions (SEDs), stars being similar to black bodies and AGN emitting energy through a power-law (Alonso-Herrero et al. 2006), the light re-emitted by dust should thus have different SEDs. Consequently, a high number of hot PAGBs in a LLAGN must produce characteristic colors in the MIR that should be clearly distinguished from those produced by an AGN.

In their study, Pastoriza et al. (2000) observed that some early-type galaxies with weak emission lines have a "blue" SED in the optical and infrared. They consequently suspected that either an AGN or PAGBs produced these blue SEDs. However, based on their MIR data they were unable to distinguish between a black body and a power law. Nonetheless, these authors concluded in favor of the PAGB hypothesis because they did not observe an excess of infrared emission, which they assumed must be a characteristic of any AGNs in the MIR. However, the sample in Pastoriza et al. (2000) was too small (only 28 galaxies) to establish what are the "normal" MIR characteristics of NELGs with different activity types, and these authors did not compare the MIR emission of their galaxies with the actual MIR emission produced by PAGB stars. These shortcomings can be rectified today thanks to data from the Sloan Digital Sky Survey (York et al. 2000) and the Wide-field Infrared Survey Explorer (WISE; Wright et al. 2010).

2. SELECTION OF THE SAMPLES

2.1. *The "standard" NELGs and the LLAGN candidates*

To establish what are the normal characteristics of galaxies with different activity types in the MIR, we have assembled a large sample of "standard" NELGs,

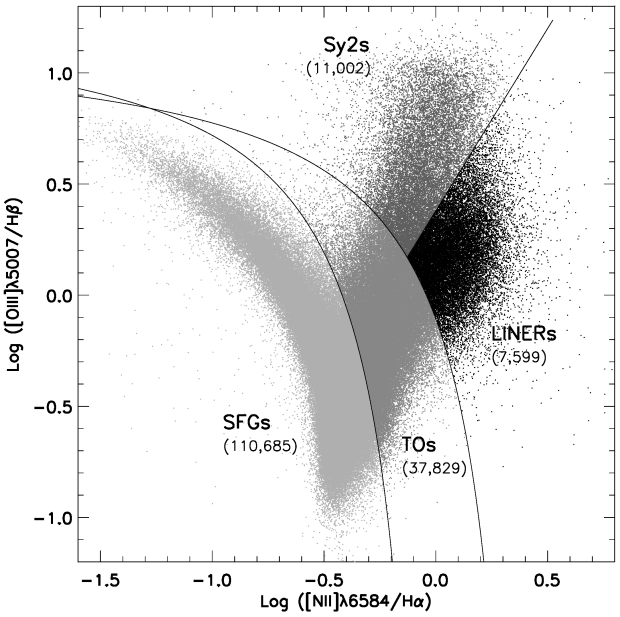

Fig. 1. The BPT-VO diagnostic diagram for the SDSS standard NELGs. The separation between SFGs and TOs was suggested by Kauffmann et al. (2003) and the separation between AGNs and TOs by Kewley et al. (2001). The separation between the LINERs and Sy2s was established in Torres-Papaqui et al. (2012a).

and searched for corresponding data in WISE. The "standard" NELGs are defined as NELGs that can be classified using standard diagnostic diagrams. These standard NELGs were thoroughly studied by Torres-Papaqui et al. (2012a). In Figure 1 we show one standard diagnostic diagram (hereafter, the BPT-VO diagram; Baldwin, Phillips, & Terlevich 1981; Veilleux & Osterbrock 1987), that we used to separate the standard NELGs into star forming galaxies (SFGs), transition type objects (TOs), Seyfert 2 (Sy2s) and LINERs. To distinguish between LINERs and Sy2s we followed the method described by Kewley et al. (2006). The distinction between the two activity types is based on differences in the [OI]λ6300 and [SII]$\lambda\lambda$6717, 6730 emission-line intensities (Torres-Papaqui et al. 2012a).

The NELGs for our study were selected from the main spectral catalog of the Sloan Digital Sky Survey Data Release 7 (SDSS DR7) (Abazajian et al. 2009), which represents the completion of the SDSS project, a series of three interlocking imaging and spectroscopic surveys, carried out over an eight-year period with a dedicated 2.5 m telescope located at Apache Point Observatory in Southern New Mexico. The SDSS DR7 catalog includes the spectra of 9.3×10^5 galaxies, 1.2×10^5 quasars and 4.6×10^5 stars[4].

As a first selection criterion we kept only the galaxies with redshift $z \leq 0.25$. Then, after correcting for the redshifts and subtracting stellar templates pro-

[4] http://www.sdss.org/dr7/start/aboutdr7.html.

duced by STARLIGHT (Cid Fernandes et al. 2005), we applied the signal-to-noise (S/N) criteria adopted by Brinchmann et al. (2004), Kewley et al. (2001, 2006), Kauffmann et al. (2003) and (Cid Fernandes et al. 2010): we kept only the galaxies that have line ratios in emission with S/N $\geq$ 3, and S/N $\geq$ 10 in the adjacent continuum.

For the MIR data, we cross-correlated the positions of the NELGs in our sample with objects in the catalog produced by WISE (Wright et al. 2010), which is available through the IRSA (IR Science Archive)[5]. Using a radius of one arcsecond around the positions of the galaxies, our search produced 110685 SFGs, 37829 TOs, 11002 Sy2s and 7599 LINERs. The results of our search were confirmed independently using the X-Match pipeline in VizieR (Ochsenbein, Bauer & Marcout 2000). Our selected galaxies have WISE fluxes with signal to noise S/N > 2 (corresponding to quality flags ph_qual equal to A, B or C) in all of the four MIR bands of WISE (3.3, 4.6, 12, and 22 μm).

To test the PAGB hypothesis we have also selected from SDSS DR7 a sample of LLAGN candidates. In Coziol et al. (1998) the LLAGNs were characterized by their spectra as galaxies that show, after a stellar template subtraction, high ratios of [NII]λ6584/Hα typical of AGNs, but that cannot be classified using standard diagnostic diagrams, because either Hβ or [OIII]λ5007, or both emission lines are undetected.

From the SDSS DR7 spectroscopic catalog we first selected 476841 NELGs with a S/N $\geq$ 10 in the continuum and redshift $z \leq 0.25$. After having corrected for the redshifts and subtracted stellar templates produced by STARLIGHT, we found 10926 galaxies with both Hβ and [OIII] undetected (hereafter identified as LLAGNα), 20784 galaxies with Hβ detected but [OIII]λ5007 undetected (identified as LLAGNβ), and 61290 galaxies with [OIII] detected but Hβ undetected (identified as LLAGNγ). Together, these three samples represent about 20% of the whole sample of NELGs. Keeping only the NELGs that have a S/N $\geq$3 in the remaining emission lines reduces the sample to 219375 galaxies (46% of the original sample). In this sample we distinguish 4198 LLAGNα, 12378 LLAGNβ and 36524 LLAGNγ, which represents $\sim$24% of the NELGs with S/N $\geq$3. After cross-correlating the positions of these galaxies with those of the objects in the WISE catalog, applying the same search radius and quality criterion on the fluxes as for the standard NELGs, we found 2840 LLAGNα, 9615 LLAGNβ, and 31467 LLAGNγ (83% of the LLAGN candidates with S/N $\geq$ 3). Counting only the NELGs with WISE data (176115 standard NELGs and 43922 LLAGN candidates), the NELGs with undetected emission represent 21% of the whole sample. Contrary to what was stated in Cid Fernandes et al. (2010), the fact that the fraction of NELGs with undetected lines stays constant suggests that the reason why some emission lines are not detected in these galaxies is not due to a low S/N (see discussion in § 2.2 below).

[5] http://irsa.ipac.caltech.edu/cgi-bin/Gator/nph-scan?mission=irsa\&submit=Select\&projshort=WISE.

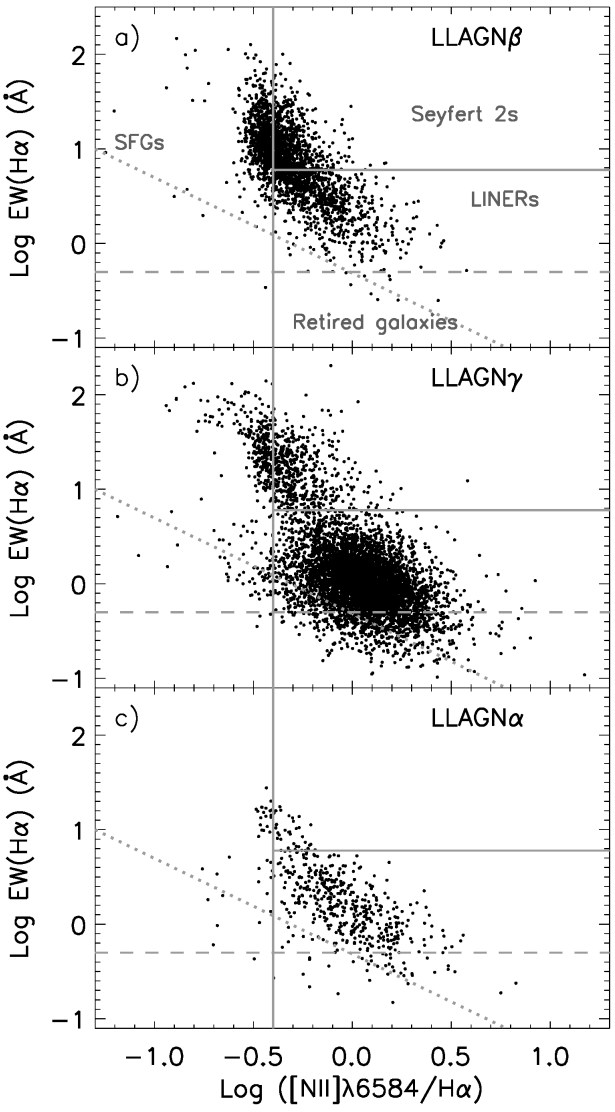

Fig. 2. WHAN diagnostic diagrams for our three samples of NELGs with some emission lines undetected: a) 9615 LLAGNβ, b) 31467 LLAGNγ, and c) 2840 LLAGNα (see descriptions in the text). The separations between the activity types are as defined in Cid Fernandes et al. (2010).

2.2. *Classification of LLAGNs according to the WHAN diagnostic diagram*

According to Cid Fernandes et al. (2010, 2011) it is possible to determine the nature of the activity of NELGs that have weak or undetected emission lines based on a new diagnostic diagram, the WHAN diagnostic diagram, that compares the EW of Hα with the

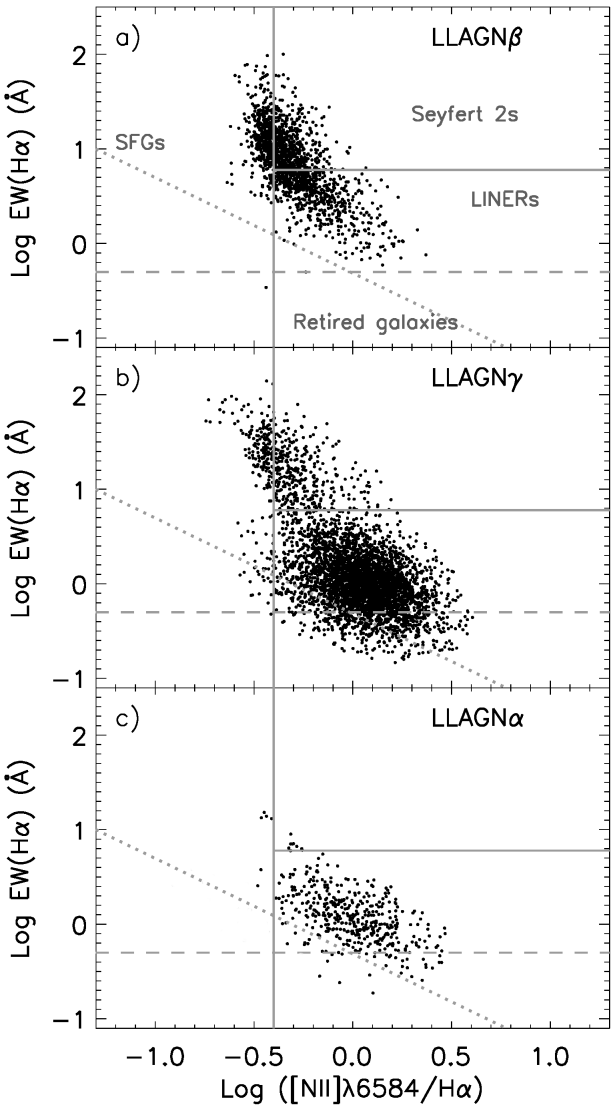

Fig. 3. Same as Figure 2 keeping only the NELGs with S/N $\geq$ 5.

ratio [NII]λ6584/Hα. Applying this diagram for a large sample of these galaxies taken from SDSS, these authors concluded that most of them are "retired galaxies", that is galaxies where the activity is dominated by PAGBs.

In Figure 2 we show the WHAN diagrams for our three samples of LLAGN candidates. In Figure 2a the LLAGNβ sample seems to form a mixture of SFGs, Sy2s and LINERs. In Figure 2b, the LLAGNγ sample shows even more diversity: a small number look like a mixture of SFGs and Sy2s, a higher fraction look like LINERs, and only a few look like retired galaxies. In Figure 2c the LLAGNα sample seems to be mostly composed of LINERs. Consequently, there seem to be very few LLAGNs in our sample consistent with the PAGB hypothesis.

From the above results, one could worry that the definition of retired galaxies is sensitive to noise introduced by the choice of a too low S/N selection criterion (e.g. Rola & Pelat 1994). To test this hypothesis, we have changed our criterion, keeping only the NELGs with S/N $\geq$ 5. The number of LLAGNγ decreases to 82% of the original sample with S/N $\geq$ 3, the number of LLAGNβ to 77.0% and the number of LLAGNα to 74.0%. However, in the WHAN diagram for the LLAGNs with S/N $\geq$ 5 shown in Figure 3, we can still identify a good fraction of LLAGNγ as retired galaxies. Also, our description in terms of mixture of activity types stays the same. This result confirms that the reason why some emission lines are not detected in these galaxies is not due to low S/N. For the rest of our analysis we will thus keep our original sample with S/N $\geq$ 3.

For comparison sake, we trace in Figure 4 the WHAN diagram for the standard NELGs classified as Sy2s and LINERs. Here we can observe that although in the BPT-VO diagram we can discriminate between the LINERs and the Sy2s, the two classes strongly overlap in the WHAN diagram. The difference comes from the use in the WHAN diagram of the EW, which is sensitive to the stellar populations and morphologies of the galaxies, but not to the ionization state of the gas or the nature of their ionizing source, which is related to the ratio of the emission lines [NII]λ6584/Hα. According to the standard definition, Sy2s are AGNs (they show high [NII]λ6584/Hα ratios) with high ionization states, because they have high [OIII]λ5007/Hβ ratios, while LINERs are AGNs with low ionization states. This difference is not reflected in the WHAN diagram.

The situation is slightly better in Figure 5 for the SFGs, but this is because the hosts of the SFGs form a more homogeneous population, they are mostly late-type spirals. However, we also note an important overlap with the Sy2s, which does not exist in the BPT-VO diagram. The situation becomes even more ambiguous in the case of the TOs. However, according to the WHAN diagram most of these galaxies are AGNs, classified either as Sy2s or LINERs, not SFGs.

According to the WHAN diagram, it is difficult to understand why the AGN nature of our three groups of LLAGN candidates was not recognized. This is unless one also rejects the AGN nature of LINERs (e.g. Eracleous, Hwang, & Flohic 2010; Singh et al. 2013). So it seems fundamental in our analysis that we also verify the PAGB hypothesis for the LINERs (see § 4.1).

2.3. *Covering the entire post-AGB evolutionary phase*

To be able to test the PAGB hypothesis, it is important to build a sample of stars that covers all the different evolutionary stages of the post-AGBs: the genuine PAGBs (pre-PNs), the PNs and the hot white dwarfs.

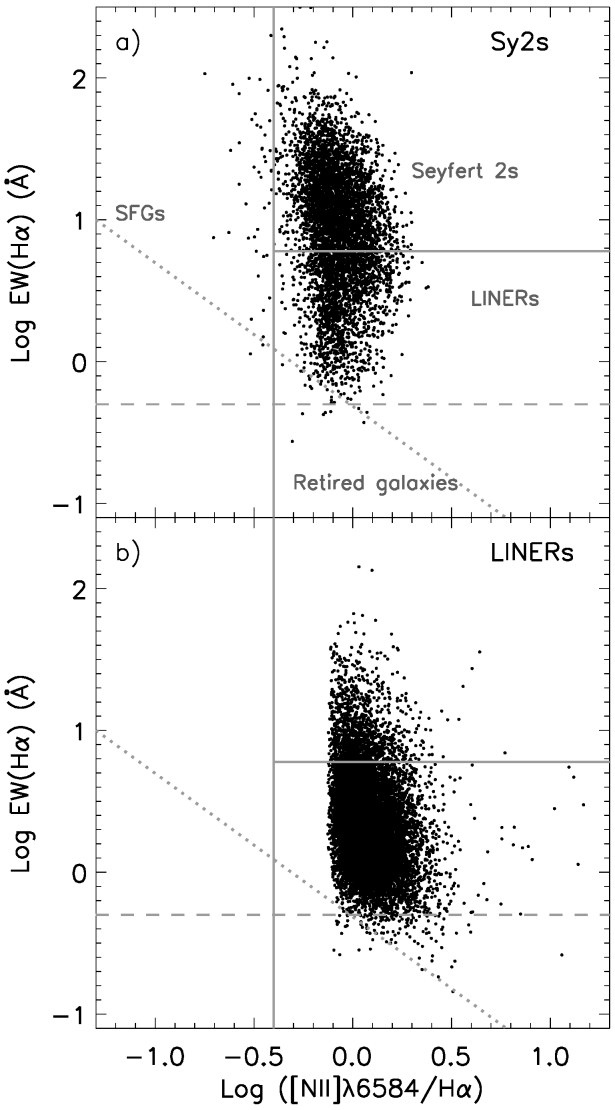

Fig. 4. WHAN diagnostic diagram for the standard NELGs: a) 11002 Sy2s and b) 7599 LINERs.

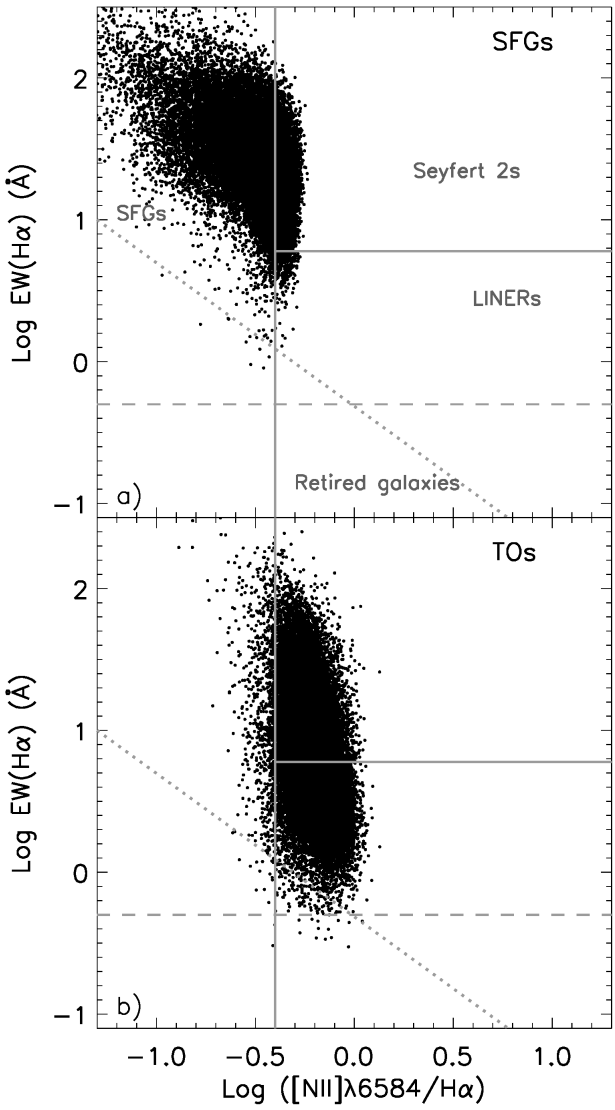

Fig. 5. WHAN diagnostic diagram for the standard NELGs: a) 110685 SFGs and b) 37829 TOs.

For the PAGBs we adopted the definition of Suárez et al. (2006) and used their list. Using a search radius of 5 arcseconds, we cross-correlated the positions of these stars with those of the objects in the WISE catalog and kept only the stars with fluxes that have S/N > 2 in all the four MIR wavebands. The spectra of these PAGBs (Suárez et al. 2006) show no emission lines, confirming that they are pre-PNs. From an original sample of 101 PAGBs, we found 76 stars satisfying our selection criteria (∼76% of the whole sample).

For the PN phase, we used the list of 492 confirmed PNs as published by Weidmann & Gamen (2011). Applying the same search and quality of flux criteria in WISE as for the PAGBs, we found 419 PNs (∼85% of the whole sample).

To complete the AGB evolutionary phase, we used the new catalog of spectroscopically confirmed white dwarf stars from SDSS DR 7 as published by Kleinman et al. (2013). There are 20407 white dwarfs in this catalog, 30% of which are hot (with an effective temperature above or equal to 18000 K). Applying the same search criteria in WISE as for the PAGBs and PNs, we found only 4056 stars (∼ 20% of the whole sample). Furthermore, all, except a few, only have upper limits in 12 and 22 μm bands. Among these 4056 "partially detected" stars, we count 1370 hot white dwarfs (∼ 33% of the sample), which implies that the "non-detection" of white dwarfs at 12 and 22 μm in WISE is independent of the effective temperature of the stars.

Our search results for the white dwarfs suggest that many of these stars are either completely free of dust, or that collectively their light is too diluted to be able to heat the dust over kpc regions in our galaxy. How-

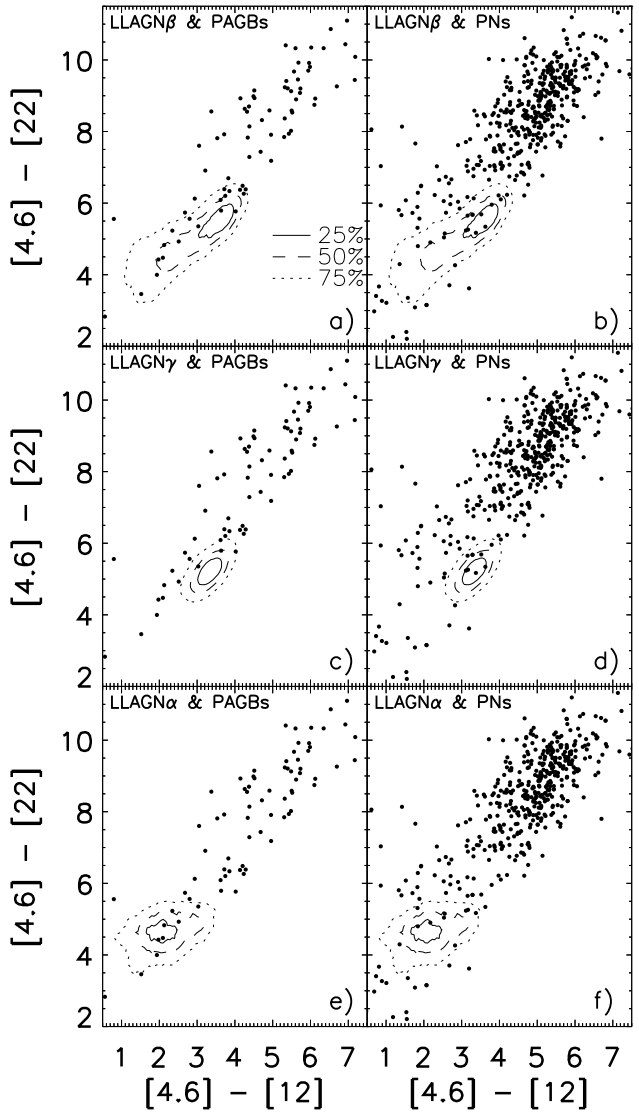

Fig. 6. MIR color-color diagrams formed by comparing the differences in magnitude between the 4.6 and 12 micron bands, with the differences in magnitude between the 4.6 and 22 micron bands. In each panel we draw the density contours (normalized to 100% at the peak density) for the galaxies, while the dots are the colors of the individual stars.

ever, this does not mean that we cannot test for the presence of hot white dwarfs in LLAGNs using MIR observations (see our discussion in § 4).

3. RESULTS: THE MIR COLORS OF LLAGNS

In Figure 6 we present the color-color diagram [4.6]-[12] vs. [4.6]-[22] for each of the different LLAGN candidate samples, and compare their MIR colors with those of the PAGBs and PNs. For the stars we show the individual colors whereas for the galaxies we trace the distribution of their colors as normalized density contours, including the corresponding fraction (25%, 50% and 75%) of galaxies in the sample around the point of maximum density (the most probable colors). The differences between the stars and galaxies in these color-color diagrams are compelling. Contrary to what is expected based on the PAGB hypothesis, only a few PAGBs and PNs have colors consistent with those of the LLAGNs. In general, the PAGBs and PNs are much redder than the LLAGNs. Note that other combinations of MIR colors yield similar results, with those of the stars significantly different than those of the LLAGNs.

In general, the colors for the stars differ from those of the LLAGNs by two important characteristics: their dispersions are much larger and their magnitudes show greater variations passing from one band to the other. This second characteristic for the stars is an indication that their MIR continua trace SEDs that are different from those of the LLAGNs (see our discussion below).

We show similar color-color diagrams for the Sy2 and LINERs in Figure 7 and for the SFGs and TOs in Figure 8. All the standard NELGs in our large sample show well defined colors, which is contrary to what is observed for the PAGBs and PNs. Although the colors of the standard NELGs are redder than those of the LLAGNs, the differences between the stars and the galaxies are still too large to be reconciled with the PAGB hypothesis. Again, using other combinations of colors yield similar results.

In Figure 9 we compare the box-whisker plots for the MIR colors of the PAGBs and PNs with those of the NELGs. The NELGs become bluer following the sequence SFGs → TOs-Sy2s-LLAGNβ → LLAGNγ → LLAGNα-LINERs. The colors of the LLAGNs and LINERs are extremely blue compared to the colors of the PAGBs and PNs. The sequence in colors observed is in direct contradiction with what is expected based on the PAGB hypothesis.

To test the statistical significance of the differences in colors, we present in Figure 10 the simultaneous 95% confidence intervals for all the pairwise comparisons of the subsample color means. These confidence intervals were obtained using the max-t test, which is based on a parametric ANOVA model (Hothorn, Bretz, & Westfall 2008; Herberich, Sikorski, & Hothorn 2010) that does not suppose the variances are the same (heteroscedasticity) or that the sizes of the samples are comparable. This test assumes the null hypothesis takes a linear form and estimates the confidence interval calculating the difference between the means in color, adding and subtracting (upper limit and lower limit) the standard error, then multiplying by the value of a t-distribution, adopting a level of confidence of 95%. A confidence interval including zero indicates no statistically signifi-

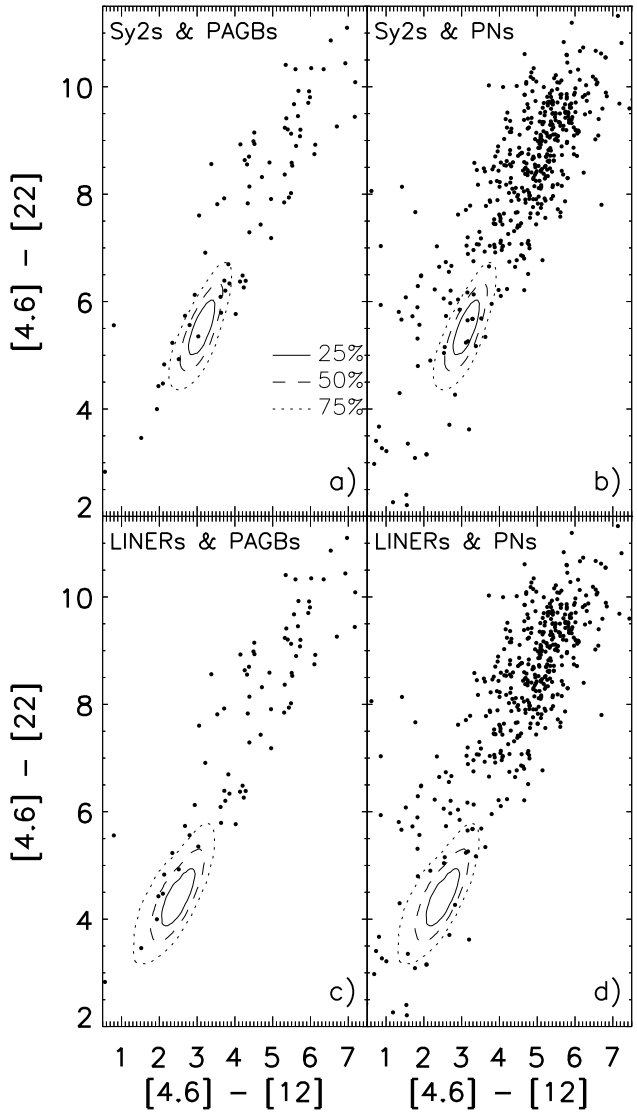

Fig. 7. Same as Figure 6 for the Sy2s and LINERs in the standard NELGs sample.

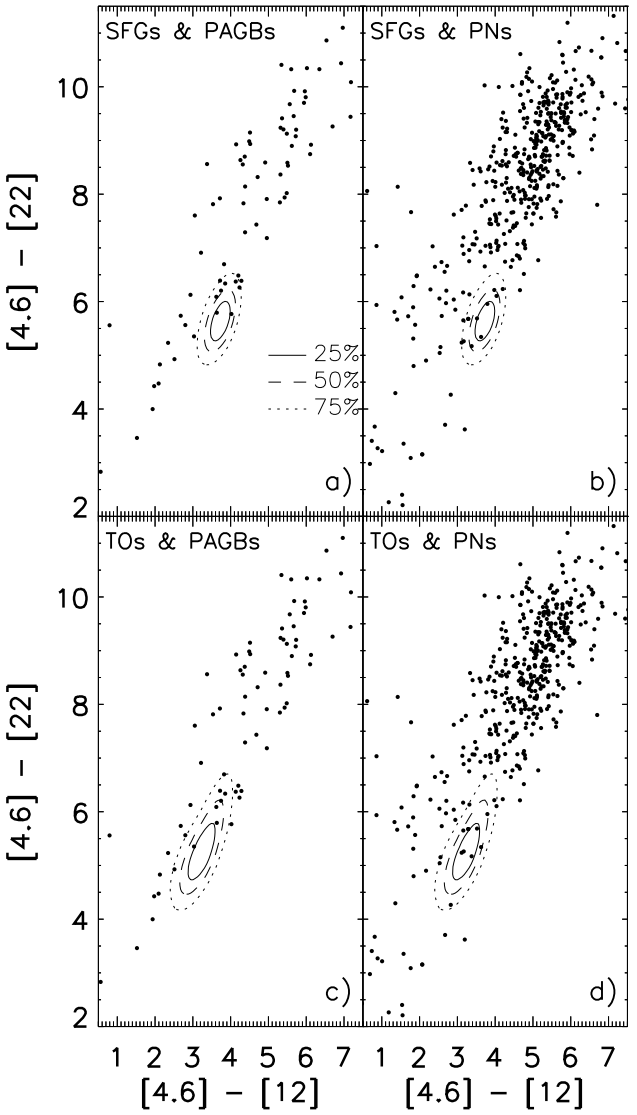

Fig. 8. Same as Figure 6 for the SFGs and TOs in the standard NELGs sample.

cant difference between the subsample means, and the farther from zero the more significant the difference.

According to the results of the max-t test presented in Figure 10 there is no significant difference on average between the colors of the PAGBs and PNs. A similar result was obtained before by Suárez et al. (2006) in the far infrared using IRAS. It is obvious from the max-t test that the NELGs, and most particularly the LINERs and LLAGNs, are too blue (all the differences are negative) to be compatible with the dominant presence of PAGBs or PNs in any of these galaxies. Based on these results, we can confidently reject the PAGB hypothesis for the LLAGNs in our sample.

The max-t tests also confirm the color sequence seen in Figure 9: the NELGs become bluer following the sequence SFGs → TOs-Sy2s → LLAGNβ → LLAGNγ → LLAGNα-LINERs. In Torres-Papaqui et al. (2013) a similar sequence was found for the standard NELGs, which was shown to trace a gradual decrease in star formation activity as the morphologies of the galaxies change from late to early types (Kennicutt 1992a,b; Coziol 1996; Coziol et al. 2011). This is supported by Figure 11, where we compare the box-whisker plots for the morphologies and EWs of Hα for all the NELGs in our sample, separated by activity types. The morphologies of the standard NELGs were determined in Torres-Papaqui et al. (2012a) and the same method was used to determine the morphologies of the three different samples of LLAGN candidates in this study. One can see that the EWs of Hα for the standard NELGs decrease following the sequence SFGs → Sy2s-TOs → LINERs. Following the same sequence these galaxies pass from late-type spirals to early-type spirals. Similarly, the EWs for the

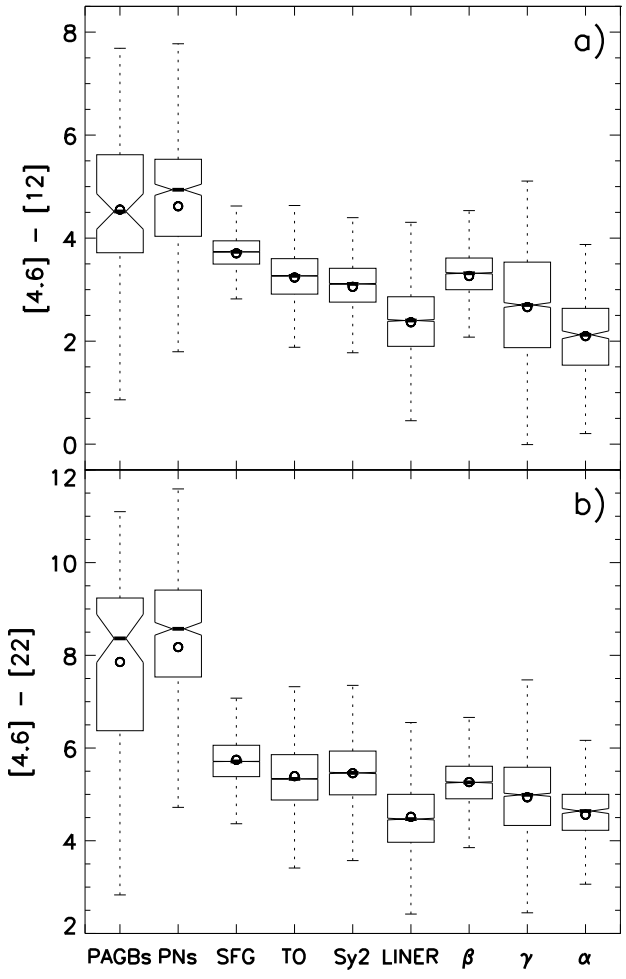

Fig. 9. Box-whisker plots comparing the two MIR colors used in our study as observed in the PAGBs, the PNs, the standard NELGs and the three LLAGN candidates, which are identified by their Greek letters. The lower side of the box is the lower quartile, Q_1, and the upper side is the upper quartile, Q_3. The whiskers correspond to $Q_1 - 1.5 \times IQR$ and $Q_3 + 1.5 \times IQR$, where IQR is the interquartile range. The median is shown as a bar and the mean as a circle. The notches have a width proportional to the IQR and are inversely proportional to the square root of the size of the sample N. Comparing two samples, no overlapping notches implies that the medians of the two samples have a high probability of being different.

three LLAGN samples decrease following the sequence LLAGNβ → LLAGNγ → LLAGNα and following the same sequence the morphologies change from late-type spirals to early-type spirals.

The above results suggest a simple physical explanation for the non-detection of some emission lines in the LLAGNs. The high ratios [NII]λ6584/Hα of the LLAGNs in the WHAN diagram suggest that these galaxies are mostly metal rich (as was previously recognized also by Cid Fernandes et al. 2010). If we could trace the BPT-VO diagram for these galaxies, most probably they would be located at the junction between the SFGs and AGNs arms of the ν shape distributions, since this is where we find the most metal rich NELGs (Coziol et al. 2011; Torres-Papaqui et al. 2012b). Therefore, the intensity of the [O III]λ5007 emission line is expected to be lower than the intensity of the Hβ emission line by a factor 3, 10 or more. This characteristic is at the basis of the explanation for the non-detection of some emission lines in NELGs.

According to the color sequence, the LLAGNβ are still actively forming stars, which suggests that their spectra are surely affected by dust absorption. Both emission lines in the blue, [OIII] and Hβ, would thus decrease in intensity. However, considering the high intensity difference, [OIII] could easily disappear while Hβ would still be observed. On the other hand, the color sequence for the LLAGNγ suggests that the star formation in these galaxies as compared to the LLAGNβ has already started to decline, which implies that these galaxies may be particularly rich in intermediate age stellar populations (Deutsch & Willner 1986; Coziol 1996; Coziol, Doyon, & Demers 2001). Since the Balmer absorption lines are culminating in intermediate age stars (Rose 1985), the Hβ emission line could completely disappear. At the same time, if the LLAGNγ have slightly lower metallicity than the LLAGNβ, then the intensity of the [OIII] lines could be sufficiently high to be detected. Finally, the color sequence for the LLAGNα suggests star formation, like in the LINERs, is at its lowest level in these galaxies. Then, in high metallicity galaxies both emission lines could easily become undetected.

We conclude therefore that a variation in star formation (Torres-Papaqui et al. 2013), in parallel with variations in morphology and metallicity explain the MIR colors sequence and the differences between the different standard NELGs and LLAGNs. According to this explanation, about 20% of the NELGs have undetected lines, because they are especially metal rich, and, as we observed, this is independent of the S/N in their spectra.

4. DISCUSSION

4.1. *Revealing the AGN nature of LLAGNs*

In the previous section we have shown that the MIR colors of the LLAGNs are significantly different from those of the PAGBs and PNs. Only a few of these stars have colors consistent with those of the LINERs and LLAGNs in our sample. However, for the PAGB hypothesis to be satisfied, the PAGBs and PNs must define the colors of the LLAGNs, which implies that their color distributions must be exactly the same. Also, considering the high number (of the order of 10^{11}) of hot white dwarfs required to explain the ionization of the gas in a typical LLAGN, it is obviously not suffi-

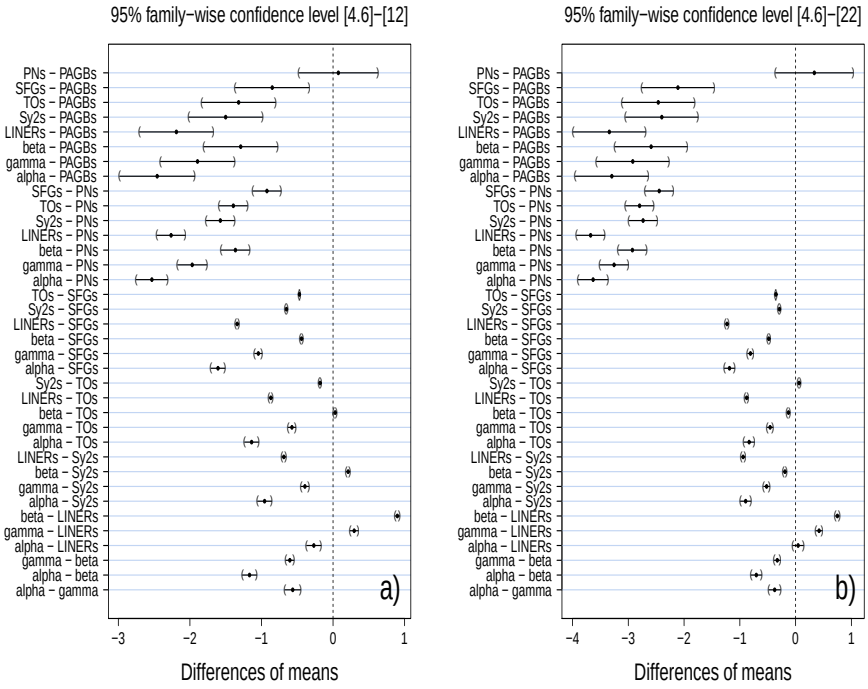

Fig. 10. The simultaneous 95% confidence intervals for all pairwise comparisons of the subsample means in colors ($\bar{C}_i - \bar{C}_j$) as obtained using the max-t test: a) for the [4.6]-[12] colors, b) for the [4.6]-[22] colors. A confidence interval including zero indicates no statistically significant difference in colors, and the farther from zero the more significant the difference. Negative differences suggest the objects in the subsample i are bluer on average than the objects in the subsample j. Comparing samples with small dispersions (small IQR) and large sample size produce small confidence intervals, making the results of the test more significant.

cient to have a few "consistent" cases, as it would imply an even higher number (higher by at least a factor 10) of special PAGBs and PNs is needed. Moreover, the few consistent cases observed are not specific to the LLAGNs or LINERs, since we can also find PAGBs and PNs that fit the Sy2s, the SFGs and the TOs. We conclude that the PAGB hypothesis cannot be maintained on the basis of the data we presented.

The difference in MIR colors between the stars and the NELGs in our sample suggests that their continua trace different types of SEDs. In Figure 12 we show the mean MIR fluxes in each band as a function of the wavelength. We see that in both the PAGBs and PNs the fluxes vary greatly as we go to higher wavelengths, suggesting that the SEDs of the PAGBs and PNs have steep slopes in the MIR. This is consistent with black bodies with high temperatures (see Figure 1 in Vickers et al. 2014). On the other hand, the fluxes show much smaller variations in the NELGs, suggesting that their SEDs in the MIR are flatter than those of the stars. For the SFGs, this is consistent with black bodies that have lower temperatures than those fitting the PAGBs and PNs (Anderson et al. 2012). For the other NELGs, however, still flatter SEDs are needed, like those typically found in AGNs (e.g. Polletta et al. 2007; Yan et al. 2013).

The MIR data are consistent with a simple model where the SEDs of the NELGs are formed by a mixture of black bodies with a low temperature typical of dust heated by O and B stars in HII regions, and power laws due to AGNs, which have flatter MIR continua than the SFGs. The relative importance of the two continuum components in NELGs is better observed in Figure 13. According to Torres-Papaqui et al. (2013) we have separated the NELGs in two groups: in a) we show the mean fluxes in the NELGs that present a high level in recent star formation (the SFGs, TOs and Sy2s) and in b) we show the flux variations in the LINERs, where star formation is presently at a very low level (the data for the Sy2s were included for comparison sake). One can see that the the variation of flux with wavelength becomes larger as the level of star formation in the galaxies increases, i.e. the SED steepens as the level of star formation in the galaxies increases. Based on the flux variations the LLAGNβ are similar to galaxies in the high star formation group, while the LLAGNγ and LLAGNα are similar to galaxies in the low star formation group. This is consistent with the classification obtained with the WHAN diagram, where it was found that the LLAGNs form a mixture of SFGs and AGNs. This result suggests that the continua vary with the amount of star formation, becoming flatter in

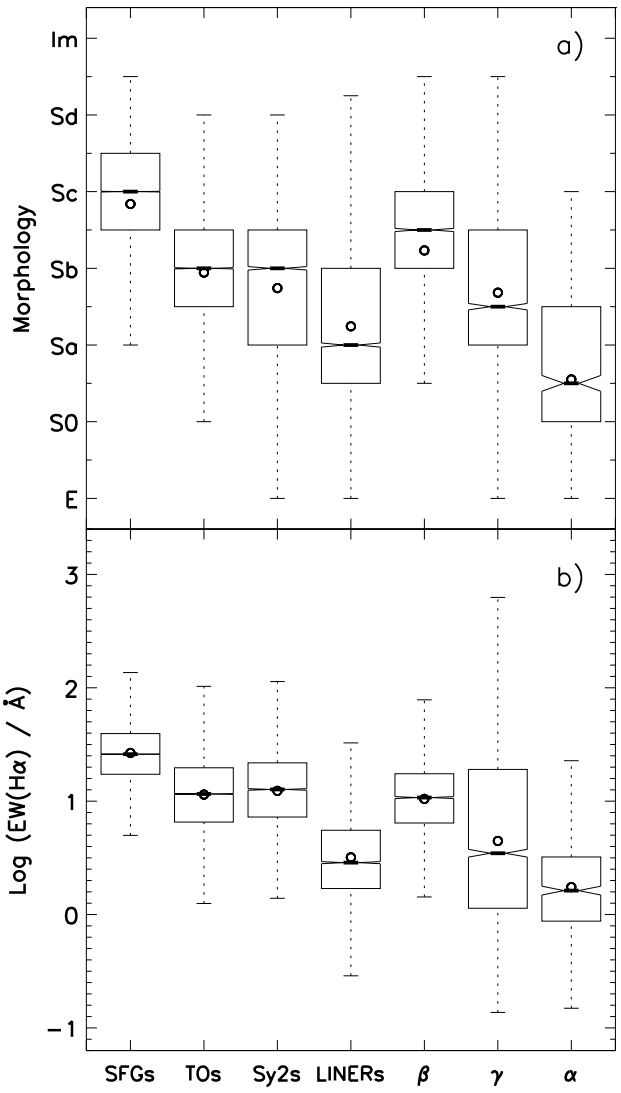

Fig. 11. Box-whisker plots comparing a) the morphologies of the NELGs in our sample, and b) their Hα EWs. The explanations for the box-whisker plots and identification of the samples are as in Figure 9.

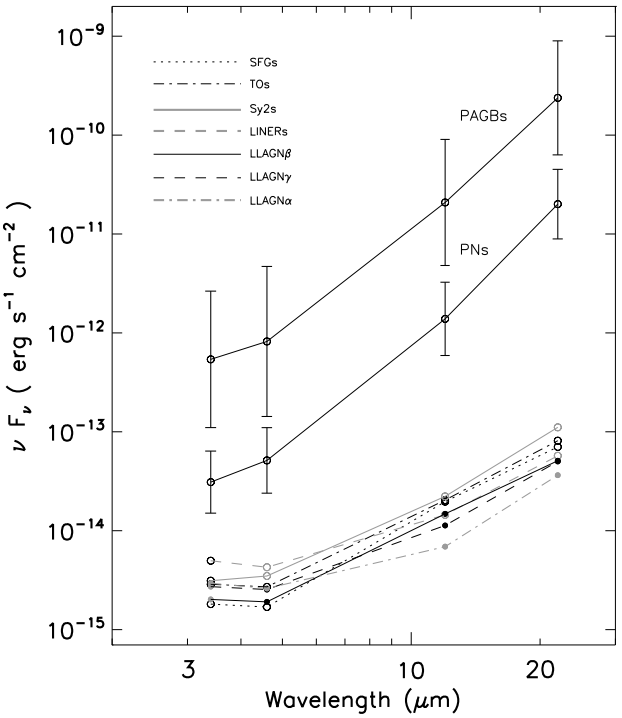

Fig. 12. The mean MIR fluxes at the four different wavelengths used by WISE. How one transforms the WISE magnitudes into fluxes is explained in Wright et al. (2010). The error bars for the stars are the errors on the means (Bevington & Robinson 2003). For clarity sake, the errors on the mean for the galaxies are shown only in Figure 12.

galaxies where the contribution of an AGN becomes predominant (Mateos et al. 2012; Donoso et al. 2012; Jarrett et al. 2013; Rosario et al. 2013).

It is easy to understand why a power law explains the trend for the colors to become bluer in the LINERs and LLAGNs. For example, consider a power law $L_\nu = C\nu^{-\alpha}$ with an exponent $\alpha = 0$, which yields fluxes independent of the wavelength. Such continuum would produce comparable MIR fluxes, and, consequently, smaller differences in magnitudes, which is consistent with the blue color trend (c.f. compare the colors of the power laws and black bodies in Table 1 of Wright et al. 2010). Therefore, we argue that due to a decreasing level of star formation in the LLAGNs and the LINERs, the continua become flatter and the MIR colors bluer, which we interpret as evidence that the power-law components due to the AGNs heating the dust in these galaxies become more apparent.

Based on the analysis described above, it should be possible to separate the NELGs according to their dominant continuum component. To verify this assumption, we present in Figure 14 the color-color diagrams [4.6]-[12] vs. [12]-[22] for the LINERs, the Sy2s and SFGs. We have also traced over the data the estimations made by Wright et al. (2010) of the colors expected in WISE for a power law with different exponents, and a black body at different temperatures. In Figure 14 one can see that the LINERs and Sy2s have colors consistent with a power law, with an exponent α varying between 0 and -1.5 in the LINERs and between -1 and -2 in the Sy2s. The SFGs on the other hand show colors that are intermediate between those produced by a power law or a black body. The variation of the [4.6]-[12] color in the NELGs with different activity types suggests that this color is sensitive to the present level of star formation in these galaxies (for similar conclusions see Mateos et al. 2012; Rosario et al. 2013).

In Figure 14 we have also included the color distribution for the PAGBs and PNs samples added to-

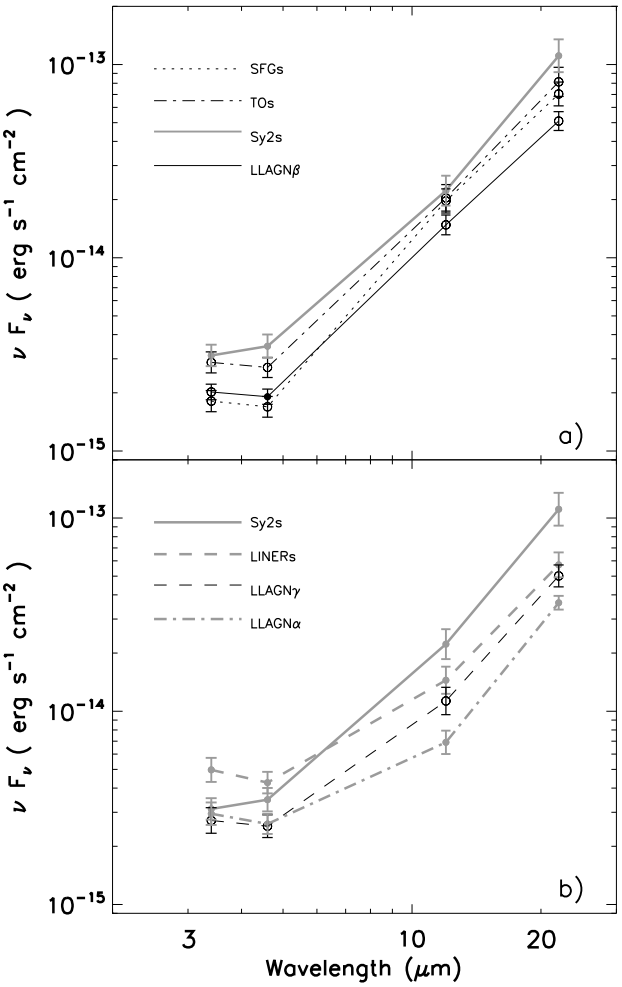

Fig. 13. Same as in Figure 12, showing in a) the NELGs with evidence of recent star forming activity and in b) the NELGs with no such evidence. The data for the Sy2s were repeated in b) for comparison sake.

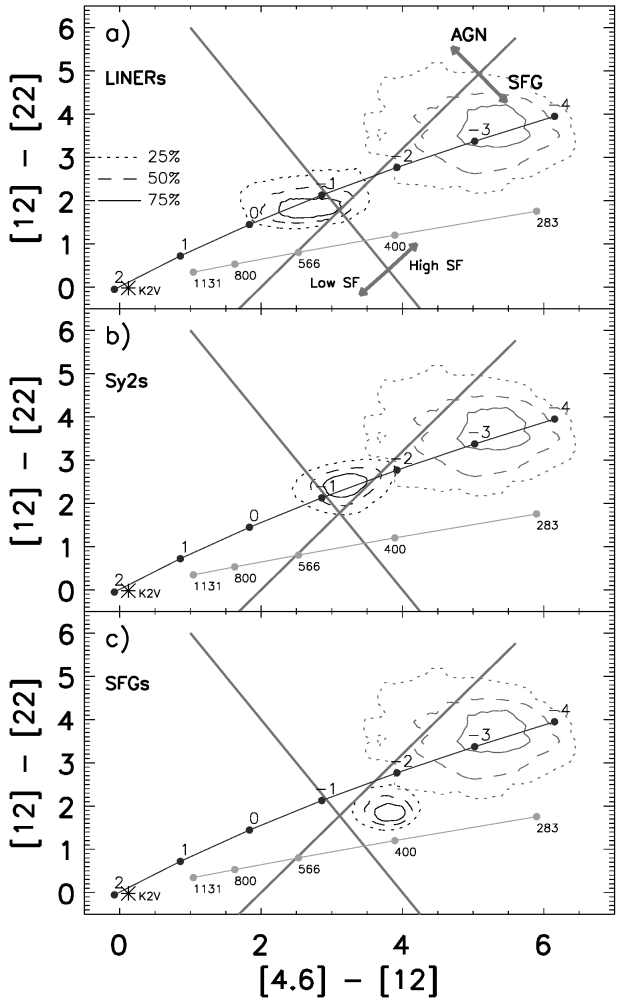

Fig. 14. New diagnostic diagram using the WISE colors. The solid line with a positive slope separates AGNs from SFGs. The solid line with a negative slope separates galaxies with high star formation activity from galaxies with low star formation activity (see explanations in the text). The positions of the LINERs, the Sy2s and SFGs are given in terms of normalized density contours, centered on the most probable colors for the activity types. For comparison sake, the density contours for the PAGBs and PNs samples added together are repeated in the three diagrams. Drawn over the data we also show the colors produced by a power law with different exponents, and a black body with different temperatures (Wright et al. 2010). As a point of reference, a star indicates the position occupied by a typical K2V star.

gether. Surprisingly their colors also seem to be fitted by a power law. This is probably due to the fact that the SEDs of these stars must be fitted by multiple black bodies with different temperatures (see Anderson et al. 2012; Vickers et al. 2014), the sum of which mimics a power law distribution. However, the power law for the PAGBs is much steeper than for the LINERs or Sy2s, the exponent α varying between -2 and -4. Consequently, the PAGBs and PNs can clearly be distinguished from the NELGs in this diagram.

According to our analysis, there is no evidence in MIR for a high number of PAGBs or PNs in the LINERs. This goes against the PAGB hypothesis, which claims that PAGBs are responsible for ionizing the gas in these galaxies. However, what can we say about the hot white dwarfs? In our galaxy these stars turned out to be undetectable in the 12 and 22 μm bands, which suggests that their SEDs must be extremely blue, falling abruptly in the MIR (e.g. Blommaert et al. 2006). The PAGB hypothesis would thus lead to a new dilemma: the source of the ionizing photons in LINERs must be different from the source of photons that heat the dust. But, from our analysis of the MIR colors, we saw that an AGN can easily explain the colors of the LINERs, and if an AGN exists in these galaxies, then this AGN can also be the source of the

ionizing photons, which makes the PAGB hypothesis redundant.

Alternatively, one can suggest, without direct observational evidence, that the hot white dwarfs somehow are also responsible for heating the dust in the LINERs. After all, some PAGBs and PNs in our analysis do reproduce the MIR colors of some of the NELGs in our sample (note, however, that the colors are not specific to one activity type) and one could propose to identify the SEDs of these special cases with the typical SEDS of hot white dwarfs in LINERs. However, there are many problems with this hypothesis. For example, reproducing the flat SEDs required to explain the LINERs in our sample implies black bodies that have lower temperatures than those of O and B stars in the SFGs. But the huge amount of ionizing photons necessary to explain the ionized gas in a typical LLAGN constitutes a strong constraint on the temperature of the stars, and the temperature cannot be lowered arbitrarily without increasing significantly the number of hot white dwarfs. Alternatively, one may assume very different distributions for the gas and the dust, namely large dust free ionized regions bounded by huge clouds of dust located at distances farther from the stars than the gas (the dust is not mixed homogeneously with the gas). But the relatively strong emission observed in MIR constrains the quantity of dust required, and the amount of dust cannot be increased arbitrarily either. Also, according to the current knowledge about the SEDs of PAGBs and PNs in the MIR (e.g. Anderson et al. 2012; Vickers et al. 2014) and according to our own analysis, it seems difficult to contrive a simple scenario that would fit specifically the SEDs of the LLAGNs based on the SEDs of hot white dwarfs. To explain the MIR colors of the LINERs, therefore, the white dwarf hypothesis seems more complicated, and consequenlty less credible than the AGN model.

4.2. *Defining a new diagnostic diagram in MIR: the AGN nature of LLAGNs*

We can use the color-color diagram in Figure 14 as a new diagnostic diagram. The physical justification for the two empirical separations shown in this diagram is the following: the NELGs with different activity types can be distinguished based on their dominant continuum component and based on their present level of star formation (Torres-Papaqui et al. 2013; Rosario et al. 2013). Consequently, we have traced in Figure 14 a diagonal (with a positive slope) that separates the SFGs from the AGNs, and another diagonal (with a negative slope) that separates the AGNs with low star formation activity (LINERs) from the AGNs with high star formation activity (Sy2s). Note that to define the different activity zones we have used only the MIR fluxes with S/N ≥ 3 (corresponding to quality flags, ph_qual, equal to A or B, in all of the four WISE bands). The

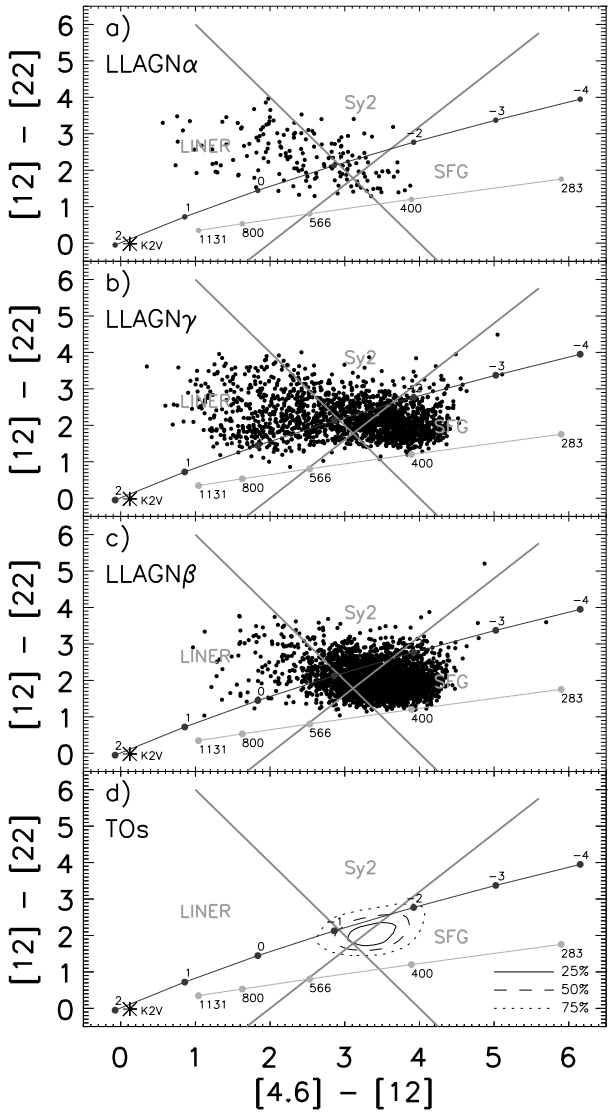

Fig. 15. The MIR diagnostic diagram for a) the LLAGNα, b) the LLAGNγ, c) the LLAGNβ, and d) the TOs.

density contours suggest that one can only obtain a probability of about 50% percent for the separation between LINERs and Sy2s. However, according to this diagram the probability that a SFG could be mistaken as an AGN is smaller than 25%. In fact, the probability that a SFG could be mistaken as an AGN is zero, if one considers the different [NII]λ6584/Hα ratios of these galaxies (cf. Figure 1).

In Figure 15 we show the classification obtained for the LLAGN candidates and the TOs using the new MIR diagnostic diagram. It can be seen in Figure 15a that the LLAGNα are similar to the LINERs. This suggests that they are AGNs with a low level of star formation activity. The LLAGNγ (Figure 15b), on the other hand, form a mixture of SFGs, Sy2s and LINERs, which again is consistent with our previous analysis. It

is interesting to compare the LLAGNβ in Figure 15c, with the TOs in Figure 15d. The MIR colors of the TOs suggest they are intermediate between the SFGs and AGNs. This is consistent with the standard interpretation based on the BPT-VO diagram (Kewley et al. 2001, 2006). The LLAGNβ would thus be similar to the TOs, which are LLAGNs with a high level of star formation.

Considering the color sequence traced by the LLAGNs in Figure 15, we see that as the [4.6]-[12] color decreases, the colors of the LLAGNs become similar to those of the LINERs, i.e. there is a clear change of colors from those produced by black bodies in SFGs to those consistent with power laws in AGNs. Because the [4.6]-[12] color is sensitive to the present level of star formation, we believe highly probable that as the star formation decreases in the LLAGNs, their MIR colors will change for those of the LINERs (Lee et al. 2007; Wang & Wei 2008; Chen et al. 2009, 2010; Yuan et al. 2010; Torres-Papaqui et al. 2012a; Zhang et al. 2013; Torres-Papaqui et al. 2013). Consequenlty, we conclude that what distinguishes the different LLAGNs in our sample is their different levels of star formation. When the star formation activity is high, the LLAGNs look like TOs, and when the star formation is declining they look like Sy2s or LINERs, which are all AGNs. Therefore, the PAGB hypothesis is also unnecessary in the case of the LLAGNs.

In general, the results obtained using the new MIR diagnostic diagram are consistent with those obtained with the BPT-VO diagram for the standard NELGs and the WHAN diagram for the LLAGNs. However, according to our analysis there are no more ambiguities as to the AGN nature of the LINERs, and consequently for the other LLAGNs, since there are only two main sources for heating the dust, namely massive stars and AGNs (Wright et al. 2010; Jarrett et al. 2011; Mateos et al. 2013; Assef et al. 2013). The MIR diagnostic diagram also suggests that these two mechanisms are frequently working at the same time (Ho, Filippenko, & Sargent 1997; Wu et al. 1998; Maoz 1999; Vila-Vilaro 2000; Kewley et al. 2001; Carter et al. 2001; Chen & Zhang 2006; González Delgado et al. 2008; Yuan et al. 2010; Carpineti et al. 2012). Indeed, what distinguishes the LINERs, the Sy2s and SFGs and explains the distributions of the LLAGNs in the MIR diagnostic diagram is their different levels of star formation (Lee et al. 2007; Wang & Wei 2008; Chen et al. 2009, 2010; Yuan et al. 2010; Torres-Papaqui et al. 2012a; Zhang et al. 2013; Torres-Papaqui et al. 2013).

Another advantage of this new MIR diagnostic diagram is that it should allow to classify different types of galaxies using the same criteria. This includes galaxies that cannot be classified using standard diagnostic diagrams, like the LLAGNs, but also radio galaxies and broad-line AGNs, like the Sy1s and the quasars.

5. SUMMARY AND CONCLUSIONS

For many authors in the field, LLAGNs do not exist. They are retired galaxies, misidentified as AGNs, where the gas is ionized by PAGB stars. However, according to the PAGB hypothesis, of the order of 10^{11} hot white dwarfs would be required to produce the right amount of ionizing photons in a typical LLAGN. Such a high number of hot stars must leave a trace not only in the optical but also in the infrared. Indeed, using MIR observations obtained with WISE we have found that an important fraction of LLAGNs are emitting in infrared and that their colors are characteristically blue. However, by comparing the MIR colors of the LLAGNs with those of the PAGBs and PNs in our galaxy, we have found that only a few of these stars have colors similar to the LLAGNs, the majority being extremely red, which contradicts the PAGB hypothesis.

The main reason why the PAGBs colors differ from those of the LLAGNs is because they have different SEDs. The SEDs of the stars in the MIR have steep slopes, while those of the LLAGNs are flatter. It is the flatness of the SEDs that produces the blue colors. These differences can be explained by assuming a black body with high temperatures in the PAGBs and a mixture in the LLAGNs of black bodies at low temperature, consistent with dust heated by O and B stars in HII regions, and different power laws due to AGNs, which have flatter MIR continua than the SFGs. As the level of star formation in the LLAGNs decreases, their continua become flatter, which we interpret as evidence that the power-law components due to the AGNs heating the dust in these galaxies become more apparent.

Consistent with the AGN model, we have shown that in a color-color diagram the LINERs and Sy2s have colors consistent with a power law with an exponent α varying between 0 and -1.5 in the LINERs and between -1 and -2 in the Sy2s. Surprisingly we have also found the colors of the PAGBs to follow a power law, but with a much steeper exponent than for the AGNs. We have also shown that the variation of the [4.6]-[12] color allows to distinguish between the NELGs with different activity types, which suggests that this color is sensitive to the present level of star formation in these galaxies.

We conclude, therefore, that the MIR characteristics of the LINERs and of the other LLAGNs in our sample are consistent with the view that they are genuine AGNs (Heckman 1980; Osterbrock & Dahari 1983; Ho et al. 1993; Barth et al. 1998; Satyapal et al. 2004; Sarzi et al. 2005; Kewley et al. 2006; Filho et al. 2006; Chen & Zhang 2006; González-Martín et al. 2006, 2009; Kauffmann 2009; Coziol et al. 2011; Torres-Papaqui et al. 2012a, 2013). If an AGN is responsible for heating the dust in these galaxies, then this AGN may also

be responsible for ionizing the gas, which makes the PAGB hypothesis unnecessary.

The LLAGNs show a large variation in their level of star formation, which explains their different characteristics. However, the MIR color sequence suggests that as the star formation decreases in these galaxies, they may all resemble the LINERs. Therefore, we also conclude that galaxies with a LINER spectral characteristic are akin to evolved or dying quasars (Heckman 1980; Kauffmann 2009; Coziol et al. 1998; Richstone et al. 1998; Miller et al. 2003; Gavignaud et al. 2008).

Thanks to our analysis we have found a new diagnostic diagram in the MIR that confirms the classification obtained using the BPT-VO diagram by eliminating the ambiguity as to the AGN nature of the LINERs. Another important advantage of this new diagnostic diagram is that it allows to determine the nature of the activity in any type of galaxies using the same criteria. This includes galaxies that cannot be classified using standard diagnostic diagrams, like the LLAGNs and the many radio galaxies, as well as broad-line AGNs like the Sy1s and the quasars. This diagnostic diagram represents a powerful new addition to the panoply of tools already in use to study active galaxies.

We thank an anonymous referee for making comments and suggestions that helped us to improve the quality of our study and its presentation. J.P. T.-P. acknowledges PROMEP for grant 103.5-10-4684, and DAIP for grant DAIP-Ugto (0432/14). This research has made use of the VizieR catalogue access tool, CDS, Strasbourg, France: (`http://vizier.u-strasbg.fr/`). This publication made use of data products from the Wide-field Infrared Survey Explorer (WISE), which is a joint project of the University of California, Los Angeles, and the Jet Propulsion Laboratory/California Institute of Technology, funded by the National Aeronautics and Space Administration. The funding for Sloan Digital Sky Survey (SDSS) has been provided by the Alfred P. Sloan Foundation, the Participating Institutions, the National Science Foundation, and the U.S. Department of Energy Office of Science. The full acknowledgement can be found here: `http://www.sdss3.org/`.

REFERENCES

Abazajian, K. N. et al. 2009, ApJS, 182, 543
Alonso-Herrero, A. et al. 2006, ApJ, 640, 167
Anderson, L. D., Zavagno, A., Barlow, M. J., García-Lario, P., & Noriega-Crespo, A. 2012, A&A, 537, A1
Assef, R. J. et al. 2013, ApJ, 772, 26
Baldwin, J. A., Phillips, M. M., & Terlevich, R. 1981, PASP, 93, 5
Barth, A. J., Ho, L. C., Filippenko, A. V., & Sargent, W. L. W. 1998, ApJ, 496, 133
Bevington, P. R., & Robinson, D. K. 2003, Data reduction and error analysis for the physical sciences, McGraw-Hill
Bianchi, L., et al. 2011, MNRAS, 411, 2770
Binette, L., Magris, C. G., Stasińska, G., & Bruzual, A. G. 1994, A&A, 292, 13
Brinchmann, J., Charlot, S., White, S. D. M., et al. 2004, MNRAS, 351, 1151
Blommaert, J. A. D. L., Groenewegen, M. A. T., Okumura, K., et al. 2006, A&A, 460, 555
Carter, B. J., Fabricant, D. G., Geller, M. J., Kurtz, M. J., & McLean, B. 2001, ApJ, 559, 606
Carpineti, A., Kaviraj, S., Darg, D., et al. 2012, MNRAS, 420, 2139
Chen, P. S., & Zhang, P. 2006, AJ, 131, 1942
Chen, X. Y., Liang, Y. C., Hammer, F., Zhao, Y. H., & Zhong, G. H. 2009, A&A, 495, 457
Chen, X. Y., Liang, Y. C., Hammer, F., et al. 2010, A&A, 515, A101
Cid Fernandes, R., Mateus, A., Sodré, L., Stasińska, G. & Gomes, J. M. 2005, MNRAS, 358, 363
Cid Fernandes, R., et al. 2010, MNRAS, 403, 1036
Cid Fernandes, R., Stasińska, G., Mateus, A., & Vale Asari, N. A. 2011, MNRAS, 413, 1687
Coziol, R. 1996, A&A, 309, 345
Coziol, R., Barth, C. S., & Demers, S. 1995, MNRAS, 276, 1245
Coziol, R., Doyon, R. & Demers, S. 2001, MNRAS, 325, 1081
Coziol, R., Ribeiro, A. L. B., de Carvalho, R. R., & Capelato, H. V. 1998, ApJ, 493, 563
Coziol, R., Torres-Papaqui, J. P., Plauchu-Frayn, I., Islas-Islas, J. M., Ortega-Minakata, R. A., Neri-Larios, D. M., & Andernach, H. 2011, RMxAA, 47, 361
Davis, C. J., Smith, M. D., Gledhill, T. M. & Varricatt, W. P. 2005, MNRAS, 360, 104
Deutsch, L.K., & Willner, S. P., 1986, ApJ, 306, L11
Donoso, E., Yan, L., Tsai, C., et al. 2012, ApJ, 748, 80
Eisenstein, D. J., et al. 2006, ApJS, 167, 40
Eracleous, M., Hwang, J. A., & Flohic, H. M. L. G. 2010, ApJ, 711, 796
Filho, M. E., Barthel, P. D., & Ho, L. C. 2006, A&A, 451, 71
Gavignaud, I., et al. 2008, A&A, 492, 637
González-Martín, O., Masegosa, J., Márquez, I., Guerrero, M. A., & Dultzin-Hacyan, D. 2006, A&A, 460, 45
González-Martín, O., Masegosa, J., Márquez, I., Guainazzi, M., & Jiménez-Bailón, E. 2009, A&A, 506, 1107
González Delgado, R. M., Pérez, E., Cid Fernandes, R., & Schmitt, H. 2008, AJ, 135, 747
Heckman, T. M. 1980, A&A, 87, 152
Herberich, E., Sikorski, J., & Hothorn, T. 2010, PLoS ONE 5(3): e9788.doi:10.1371/journal.pone.0009788
Ho, L. C., Filippenko, A. V., & Sargent, W. L. W. 1993, ApJ, 417, 63
Ho, L. C., Filippenko, A. V., & Sargent, W.L.W. 1997, ApJS, 112, 315
Hothorn, T., Bretz, F., & Westfall, P. 2008, Biom J, 50, 346
Jarrett, T. H., et al. 2011, ApJ, 735, 112
Jarrett, T. H., Masci, F., Tsai, C. W., et al. 2013, AJ, 145, 6
Kauffmann, G., et al. 2003, MNRAS, 346, 105
Kauffmann, G. 2009, A&A, 500, 201
Kennicutt, R.C., Jr, 1992a, ApJS, 79, 255
Kennicutt, R.C., Jr. 1992b, ApJ, 388, 310

Kennicutt, R. C., Jr., Tamblyn, P., & Congdon, C. E. 1994, ApJ, 435, 22
Kewley, L. J., Dopita, M. A., Sutherland, R. S., Heisler, C. A., & Trevena, J. 2001, ApJ, 556, 121
Kewley, L.J., Groves, B., Kauffmann, G., & Heckman, T., 2006, MNRAS, 372, 961
Kitsikis, A. 2007, Ph. D. Thesis, University Munich, Germany
Kleinman, S. J., et al. 2013, ApJS, 204, 5
Kwok, S. 2000, The origin and evolution of planetary nebulae (Cambridge University Press)
Lee, J. H., Lee, M. G., Kim, T., et al. 2007, ApJL, 663, L69
Madau, P., Pozzetti, L., & Dickinson, M. 1998, ApJ, 498, 106
Maoz, D. 1999, Adv. Space Res., 23, 855
Martínez, M.A., del Olmo, A., Coziol, R., & Focardi, P. 2008, ApJ, 678, L9
Martínez, M.A., del Olmo, A., Coziol, R., & Perea, J. 2010, AJ, 139, 1199
Mateos S., et al. 2012, MNRAS, 426, 3271
Mateos, S., et al. 2013, MNRAS, 434, 941
McCook, G. P. & Sion, E. M. 1999, ApJS, 121, 1
Miller, C. J., Nichol, R. C., Gómez, P. L., Hopkins, A. M., & Bernardi, M. 2003, ApJ, 597, 142
Ochsenbein, F., Bauer, P., & Marcout, J. 2000, A&AS, 143, 23
Osterbrock, D. E., & Dahari, O. 1983, ApJ, 273, 478
Osterbrock, D. E. 1989, Astrophysics of Gaseous Nebulae and Active Galactic Nuclei, University Science Books.
Osterbrock, D. E., & Ferland, G. J. 2006, Astrophysics of Gaseous Nebulae and Active Galactic Nuclei, Second Edition, University Science Books
Pastoriza, M., Ferrari, F., Macchetto, F., & Caon, N. 2000, ASPC, 221, 95
Phillips, M. M., Jenkins, C. R., Dopita, M. A., Sadler E. M., & Binette, L. 1986, AJ, 91, 1062
Polletta, M., Tajer, M., Maraschi, L., et al. 2007, ApJ, 663, 81
Pottasch, S. R. 1965, Vis. Astr., 6, 149
Richstone, D., et al., 1998, Nature, 395, 14
Rola, C., & Pelat, D. 1994, A&A, 287, 676
Rosario, D. J., Santini, P., Lutz, D., et al. 2013, ApJ, 771, 63
Rose, J. A. 1985, AJ, 90, 1927
Sarzi, M., Rix, H.-W., Shields, J. C., et al. 2005, ApJ, 628, 169
Satyapal, S., Sambruna, R. M., & Dudik, R. P. 2004, A&A, 414, 825
Singh, R., et al. 2013, A&A, 558, 43
Stasińska, G., Vale Asari, N., Cid Fernandes, R., Gomes, J. M., Schlickmann, M., Mateus, A., Schoenell, W., & Sodré, L., Jr. 2008, MNRAS, 391, L29
Stern, D., et al. 2012, ApJ, 753, 30
Suárez, O., et al. 2006, A&A, 456, 173
Taniguchi, Y., Shioya, Y., & Murayama, T. 2000, AJ, 120, 1265
Torres-Papaqui, J. P., Coziol, R., Andernach, H., Ortega-Minakata, R. A., Neri-Larios, D. M. & Plauchu-Frayn, I. 2012a, RMxAA, 48, 275
Torres-Papaqui, J. P., Coziol, R., Ortega-Minakata R. A., & Neri-Larios, D. M. 2012b, ApJ, 754, 144
Torres-Papaqui, J. P., Coziol, R., Plauchu-Frayn, I., Andernach, H. & Ortega-Minakata, R. A., 2013, RMxAA, 49, 311
Veilleux, S., & Osterbrock, D.E., 1987, ApJS, 63, 295
Vickers, S. B., Frew, D. J., Parker, O. A., & Bojicic, I. S. 2014, arXiv:1403.7230
Vila-Vilaro, B. 2000, PASJ, 52, 305
Volk, K. M., & Kwok, S. 1989, ApJ, 342, 345
Wang, J., & Wei, J. Y. 2008, ApJ, 679, 86.
Weidmann, W. A., & Gamen, R. 2011, A&A, 526, 6
Wright, E. L., et al. 2010, AJ, 140, 1868
Wu, H., Zou, Z. L., Xia, X. Y., & Deng, Z. G. 1998, A&AS, 132, 181
Yan, L., Donoso, E., Tsai, C.-W., et al. 2013, AJ, 145, 55
York, D. G., Adelman, J., Anderson, J. E., Jr., et al. 2000, AJ, 120, 1579
Yuan, T.-T., Kewley, L. J., & Sanders, D. B. 2010, ApJ, 709, 884
Zhang, X.G., Dultzin-Hacyan, D., & Wang, T. G. 2007, MNRAS, 374, 691
Zhang, Z. T., Liang, Y. C., & Hammer, F. 2013, MNRAS, 430, 2605

H. Andernach, R. Coziol, J. M. Islas-Islas, R. A. Ortega-Minakata, and J. P. Torres-Papaqui: Departamento de Astronomía, Universidad de Guanajuato, Apdo. Postal 144, 36000, Guanajuato, Gto, Mexico (heinz, rcoziol, jmislas, rene, papaqui@astro.ugto.mx).
D. M. Neri-Larios: School of Physics, The University of Melbourne, Parkville, Vic. 3010, Australia (danielnl@student.unimelb.edu.au).
I. Plauchu-Frayn: Instituto de Astronomía, Universidad Nacional Autónoma de México, Campus Ensenada, Apdo. Postal 877, Ensenada, B.C., Mexico (ilse@astrosen.unam.mx).